Inorganic Chemistry Communications 133 (2021) 108931

Contents lists available at ScienceDirect

Inorganic Chemistry Communications

journal homepage: www.elsevier.com/locate/inoche

Phytosynthesis of *Prosopis farcta* fruit-gold nanoparticles using infrared and thermal devices and their catalytic efficacy

Muwafaq Ayesh Rabeea [a], Ghassan Adnan Naeem [b], Mustafa Nadhim Owaid [c,d,*], Azlan Abdul Aziz [e], Mahmood S. Jameel [e], Mohammed Ali Dheyab [e], Rasim Farraj Muslim [d], Lina F. Jameel [b]

[a] Department of Applied Chemistry, College of Applied Sciences-Hit, University Of Anbar, Hit 31007, Anbar, Iraq
[b] Department of Biophysics, College of Applied Sciences-Hit, University Of Anbar, Hit 31007, Anbar, Iraq
[c] Department of Heet Education, General Directorate of Education in Anbar, Ministry of Education, Hit 31007, Anbar, Iraq
[d] Department of Environmental Sciences, College of Applied Sciences-Hit, University Of Anbar, Hit 31007, Anbar, Iraq
[e] Nano-Optoelectronics Research and Technology Lab (NORLab), School of Physics, Universiti Sains Malaysia, 11800 Pulau Pinang, Malaysia

ARTICLE INFO

Keywords:
AuNPs
Catalytic
Fabaceae
Green Chemistry
IR radiation

ABSTRACT

This study is a new attempt to synthesize gold nanoparticles (AuNPs) using the extract of fresh mature fruits of the Iraqi *Prosopis farcta* plant (Fabaceae). The synthesis has been performed under infrared (IR) irradiation treatment and compared with the heating procedure at 90 °C. *P. farcta*-AuNPs has been investigated as a nanocatalyst to remove Methylene blue (MB) dye from aqueous solutions. TEM, FE-SEM, EDX, XRD, size Distribution Report by Intensity, Zeta Potential, UV–Vis, GC-Mass and FTIR have been used to characterize the synthesized AuNPs. The color transformation of colloidal AuNPs under both IR radiation and heat confirmed the efficient reduction of Au^{+} to Au^{0} and its stabilization using *P. farcta* extract. AuNPs synthesized using IR were mainly spherical with an average diameter hydrodynamic size of 25.43 nm, and Zeta Potential of −26.5 mV. While AuNPs prepared using the heating treatment showed a quasi-spherical shape with an average size of 53.12 nm and Zeta Potential of −24.4 mV. FTIR analysis indicates that phenolic compounds of *P. farcta* extract are protected in the AuNPs synthesized by IR irradiation, but they are lost in another sample. Thus, the AuNPs biosynthesized using IR radiation have higher colloidal stability, smaller size, more spherical and more preserved core–shell structure than Au NPs prepared using the heat treatment. Bionano-reduction of MB using synthesized AuNPs using IR irradiation best than synthesized using the heating procedure. This work encourages using IR irradiation as a new method to produce and improve AuNPs for catalytic handling.

1. Introduction

Nanotechnology involves modifying the size and morphology of materials in the nano-scale to advance their properties [1]. This science has been achieved in past decades through chemical [2] and physical techniques [3]. Therefore, several materials have been produced on a nano-scale, such as carbon [4], gold [5,6], silver [7–9], etc. Nonetheless, nanomaterials will be of more interest when preparing them in green or eco-friendly methods [10]; thus, alternative or innovative procedures are being developed in this field [11]. Recently, the biosynthesis of metallic nanoparticles using plant extracts [12–15], fungi [16–18], truffles/tubers [19], and bacteria [20] have been enhanced to become acceptable for medical and pharmaceutical applications as nano-drugs [21]. However, many biomaterial were used in the green synthesis of nanoparticles [22], including *Euphorbia condylocarpa* [23], leaf extract of *Euphorbia falcata* [24], *Piper longum* [25], and leaf extract of *Euphorbia thymifolia* [26], arthropods [27], *Enterococcus* [28] pigments, enzymes, agro-wastes [29], and animal waste materials [30]. Furthermore, the biomaterials-assisted mycosynthesis of gold nanoparticles have been used for the decolorization of organic dye [6,31]. The green nanomaterials were used for many usages like water treatment [32–34], reducing nitroarenes [35], reducing nitro-aromatics [36] reducing pharmaceutical residues [37] degradation of organic dyes [35,38–41], and removing pesticides from wastewater [42]. Besides, another study showed that radiolytic preparation of gold nanoparticles using charged particles allows for facile control of the nucleation process in a single

* Corresponding author.
E-mail addresses: muw88@uoanbar.edu.iq (M.A. Rabeea), mustafanowaid@uoanbar.edu.iq (M.N. Owaid).

https://doi.org/10.1016/j.inoche.2021.108931
Received 8 August 2021; Received in revised form 4 September 2021; Accepted 15 September 2021
Available online 21 September 2021

procedure [43]. Generally, using biomaterials to fabricate new greener nanoparticles is remarkable due to their low toxicity and finding bioactive organic materials around gold atoms [44].

Prosopis farcta, Fabaceae family, is a thorny shrub with an approximate height of 30–80 cm. It is native to North Africa and Southwest Asia and grows in the North American region [45]. This plant grows naturally in cultivated lands and adapts to high temperatures, high salinity, and arid conditions. The extract of *P. farcta* can be utilized as medication for injuries/lesions as well as a remedy for diabetes [46,47]. Besides, the extract from its roots has been used by Arab nations to treat hypertension and angina pectoris [48]. Harzallah-Skhiri and Jannet [49] reported that *P. farcta* is rich in flavonoids and phenolic compounds, while Persia et al. [50] asserted that it does not contain any harmful compounds.

The extract of *P. farcta* leaves was firstly used to produce Ag and Au nanoparticles in 2015 and 2018, respectively [51,52]. Recently, no study has researched the use of its fruits to reduce metallic salts to form gold nanoparticles except the synthesis of silver NPs [53] and platinum NPs [54]. Therefore, this study highlights that for the first time, the phyto-synthesis of spherical AuNPs using the extract of fresh mature fruits of *P. farcta* by including infrared (IR) irradiation, which has been compared with the heating method. In addition, the decolorization of MB in aqueous solutions using the synthesized AuNPs has been achieved.

2. Material and methods

2.1. Chemicals

Chloroauric acid (purity 99.9%), sodium borate and methylene blue dye have been purchased from Sigma Aldrich, Germany.

2.2. Samples of Prosopis farcta

Fresh mature fruits of *Prosopis farcta* (Fabaceae) are available in huge amounts in Iraq, have been collected from the local cultivated fields in Hit city, Anbar.

2.3. Preparation of Prosopis farcta extract

Here, the *Prosopis farcta* fresh mature fruits have been firstly washed with deionized water and then sliced into tiny pieces. Only 5 g of the cut fresh fruits have been added to 100 ml of deionized water in a round flask and boiled at 90 °C for 30 min. The resulted suspension has been subsequently filtered using Whatman filter paper (No. 40). The aqueous filtrate has been centrifuged at 5000 rpm for 15 min and stored in a freezer at −20 °C.

2.4. Gas chromatography-mass spectroscopy of P. Farcta crude extract

Gas chromatography-mass spectroscopy (GC-Mass) (PerkinElmer Clarus 600 t) has been utilized to distinguish biomolecular compounds in the extract of *P. farcta*. The evaporation injection procedure (10:1) has been applied. High-purity helium gas has been used as a mobile phase. The temperature of the injection system has been set at 260 °C. GC-Mass was performed using a fused silica capillary column (30 m × 0.25 mm ID). Electron ionization mass spectrometry has been achieved in areas 40–500 Da.

2.5. Synthesis of Au NPs

The synthesis of Au NPs involves two strategies. The first one involved adding 2 ml of the aqueous extract to 48 ml of 10^{-4} M trichloride hydrochloride, then boiling at 90 °C in a 250 ml-Erlenmeyer flask under constant stirring. For the second strategy, the same chemical and extract were utilized but under the effect of IR radiation (The output source of the IR light with a wavelength of 850 nm, Voltage - Forward of 31.9 V, and Current - DC Forward of 65 mA has been used in current work).

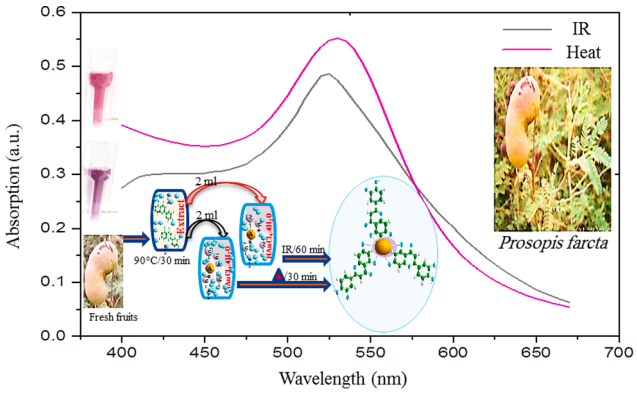

Fig. 1. UV–Vis spectrums of the phytosynthesized AuNPs.

2.6. Characterization of Au NPs

The final products were analyzed at Universiti Sains Malaysia (USM), Malaysia. UV–visible spectra of the samples were obtained using a Shimadzu dual beam spectrophotometer (AV-1800) to determine the bio-reduction of Au^{+} ions to Au^{0} in the aqueous solution. The elemental composition, morphology and size were analyzed using FESEM attached with EDX (Oxford-Instrument INCA400). The hydrodynamic particle size and zeta potential of the samples were determined using Zetasizer Ver. 7.03 (Malvern Instruments Ltd., Worcestershire, UK). XRD pattern of the samples was obtained to characterize their crystal structures using Bruker AXS D-8 powder X-ray diffractometer (operated at 40 kV and 15 mA using CuKα radiation (λ = 1.5406 A°)). The functional groups present in the samples were determined using FTIR (FTIR-JASCO 4100 Spectrometer at 4000 cm^{-1} to 400 cm^{-1}).

2.7. Degradation of methylene blue

The catalytic efficacy of synthesized Au NPs was analyzed by mixing two volumes of the colloidal AuNPs (150 μL and 200 μL, separately) with 0.5 ml of $NaBH_4$ (50 mM) and 2 ml of 10 ppm MB dye. The absorbance was checked using UV–vis in the range of 400–900 nm, while the decolorization efficiency of the dye was checked at 670 nm using the Eq. (1) [55]:

$$\text{Decolorization percentage} = (A0 - At/At)*100 \quad (1)$$

where, A0: the absorbance of MB at 0 s, At: the absorbance of MB after the incubation time (60 sec).

3. Results and discussion

Ultraviolet–visible spectrometry has been used in a range from 400 − 700 nm and the color alteration of the medium from colorless to purple have been used to confirm the nucleation of Au^{+} ions in the aqueous solution (containing $HAuCl_4{\cdot}4H_2O$ and *Prosopis farcta* extract as a reducing agent) (Fig. 1). The extract of the fresh mature fruits of *P. farcta* has been used to reduce Au ions ($HAuCl_4{\cdot}4H_2O$) to Au atoms. IR irradiation and heat have been separately used in the synthesis of AuNPs to catalyze the nucleating process. The two modification processes also changed the optical characteristics of the colloid medium. The color of the mixture transformed from colorless to light purple after 10 min, and became permanently pink after 30 min in the case of IR, while changed to light purple after 20 min, and became fixed at pink after 60 min in the case of the heat approach. Surface Plasmon Resonance (SPR) principle

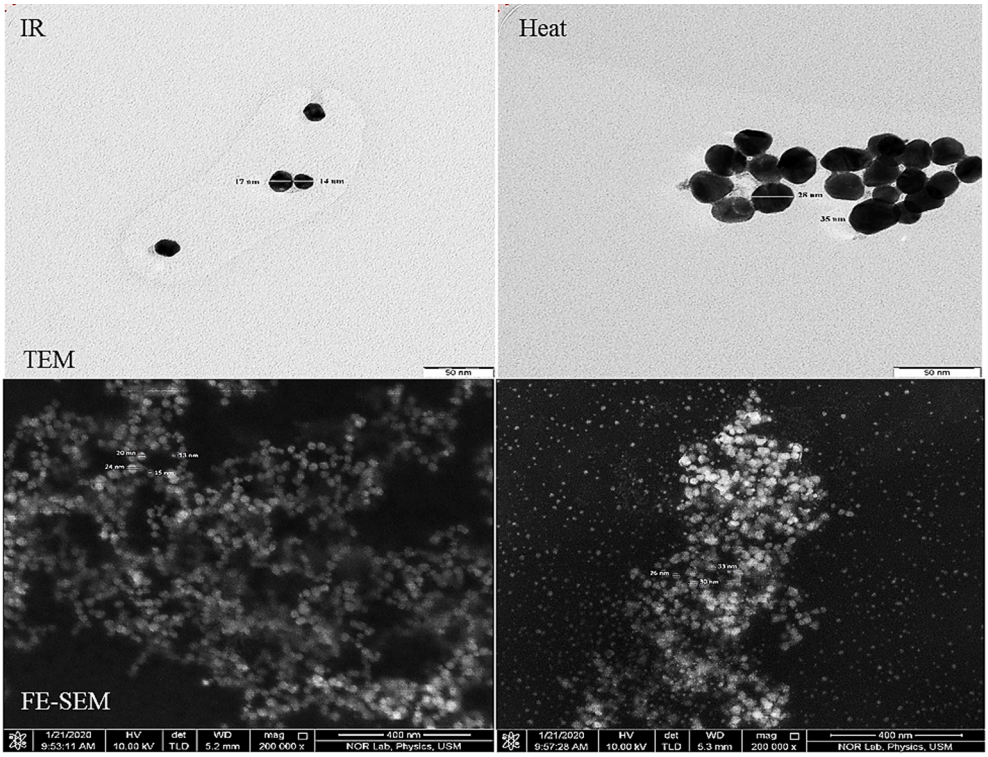

Fig. 2. TEM and FESEM images of the synthesized AuNPs by IR and heat.

describes the modulations in electronic structures of Au NPs surfaces [56]. When using heat to synthesize Au NPs, the distinct absorption band (Lambda max) at 530 nm (wide) appeared, which related to the inciting of SPR because of the reaction in the colloidal solution (Au NPs) [57]. While IR treatment exhibited Lambda max reached 525 (sharp) nm, it took more time for formation due to the low energy of IR radiation which led to the reduction of Au ions [58]. The increasing collision among organic components of the extract and ions of $HAuCl_4{\cdot}4H_2O$ releases more electrons. At the same time, the heating process lowers the activation energy (E) of the reduction reaction of the medium, thereby generating Au^0 (Eq. (2)).

$$(Heat)HAuCl_4.4H_2O + P.farcta\ \ extract \leftrightarrow^{90^\circ C} Collsion \rightarrow Au^+ \xrightarrow{e^-} Au^0 \quad (2)$$

The photoacceptor molecules (i.e. chromophores) and phenolic components in chemical precursors and the organic extract absorb IR energy which is utilized to initiate the nucleation process of AuNPs. The interaction of IR radiation with the organic molecules produces photothermal effects, which are absorbed in a photon form and converted to signals that can stimulate different processes [59,60]. Thus, the impact of IR radiation is based on the conversion of photon energy into electron emissions (photoelectric effect). Therefore, organic compounds of *Prosopis farcta* extract such as cytochrome complex can be considered as electron inducers that may change photon energy into electron liberation "caged electron" which performs the reduction process of gold ions (Eq. (3)). The polyphenol compound in the extract of *Prosopis farcta* is also served as an electron donor. The vibrational energy of IR affects the molecules by increasing their electron donation to generate slow but good orientation of controlled nanosized gold nanoparticles. Fig. 1 illustrates the IR and heat-assisted reaction between the Au ions and the organic extract.

$$IR)HAuCl_4.4H_2O + Prosopis\ \ farcta\ \ extract \rightarrow Au^+ \xrightarrow{e^-} Au^0 \quad (3)$$

Fig. 2 exhibited the transmission electron microscopy (TEM) and FESEM images of AuNPs generated under two treatments used in this work. In the AuNPs synthesis process, the average diameter of AuNPs decreased from 30 nm in the case of heat procedure to 15 nm by IR

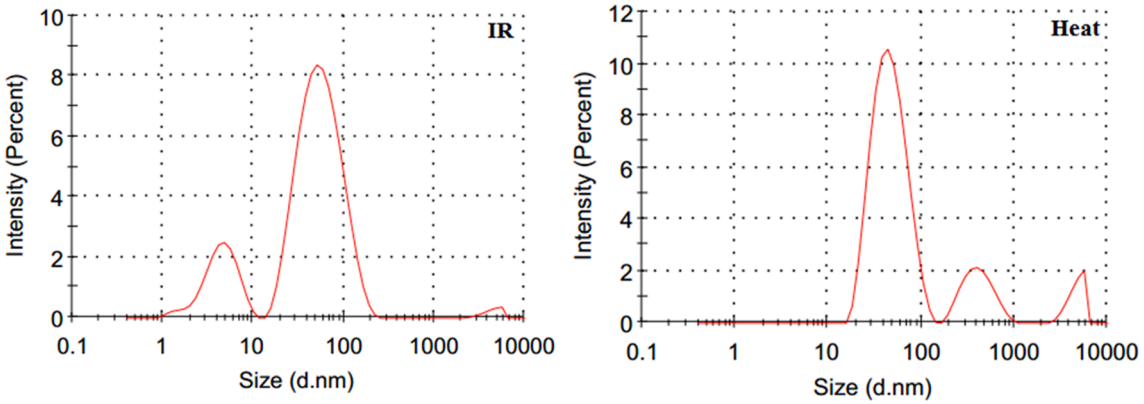

Fig. 3. Size Distribution of synthesized AuNPs by IR and heat approaches.

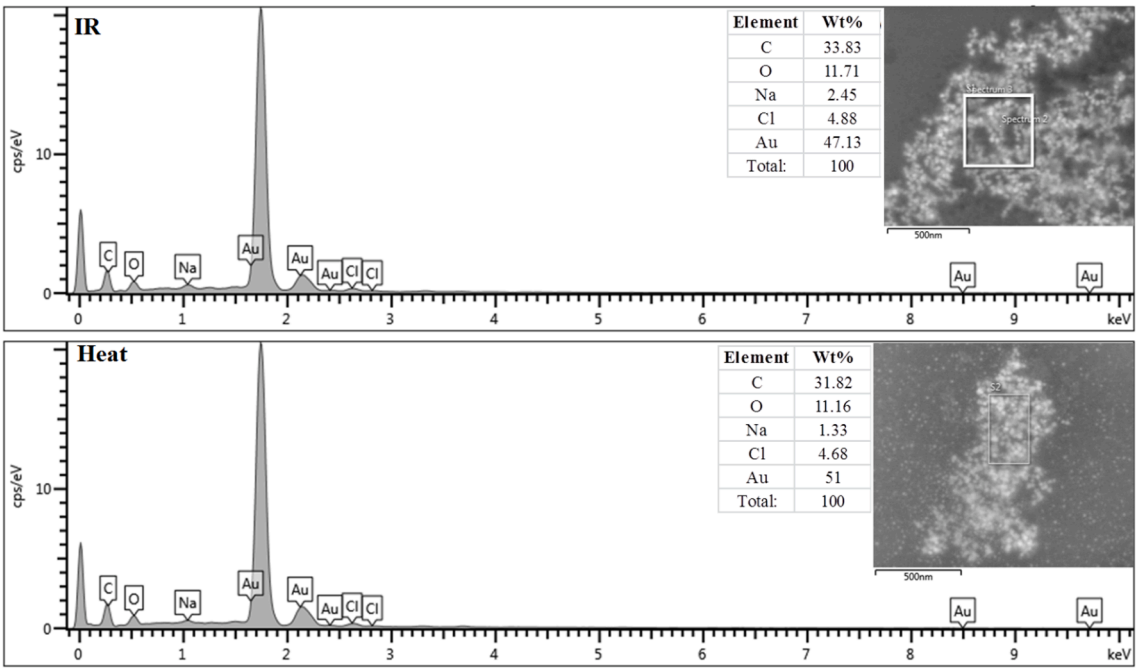

Fig. 4. EDX image of the synthesized AuNPs by IR and heat.

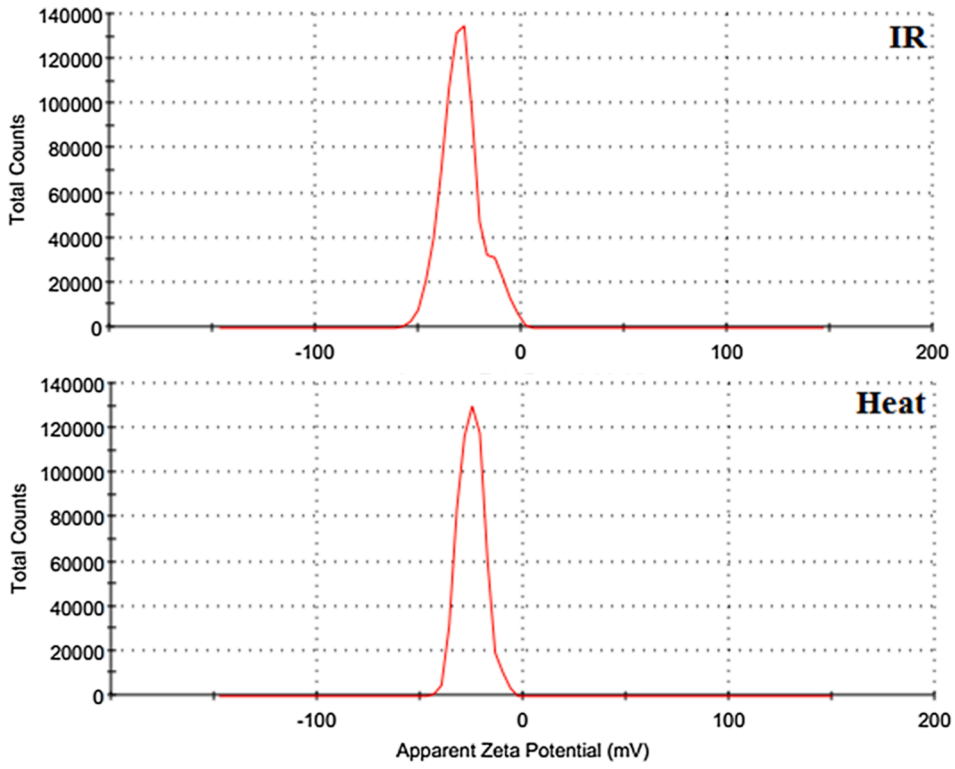

Fig. 5. Zeta Potential of the synthesized AuNPs by IR and heat.

approach, as seen in Fig. 3, which showed the distribution of the synthesized Au NPs. The quasi-spherical shape of the Au NPs synthesized under IR irradiation with an average real diameter, as in FESEM (Fig. 2-IR), between 13 nm and 24 nm that confirmed the reduction of Au^{+} to Au^{0} in the aqueous phase. Besides, Fig. 3-IR showed the Z-Average (d.nm) hydrodynamic size of Au NPs reached 25.43 nm; lesser size particles were also observed with some particles sized approx. 15 nm. Conversely, shapes of Au NPs synthesized under the heating procedure were spherical with Z-Average (d.nm) of 53.12 nm, with larger sized particles also observed (Fig. 3-Heat); FESEM (Fig. 2-Heat) exhibited real diameter averaged between 26 nm and 33 nm.

The disparity in morphology and particle size indicates that the low energy of IR radiation affects the spatial distribution of compounds in the medium, thereby influencing the nucleation process and transformation of the particles into lesser-sized nanoparticles compared to the heat procedure. The absorption of IR radiation by the aqueous

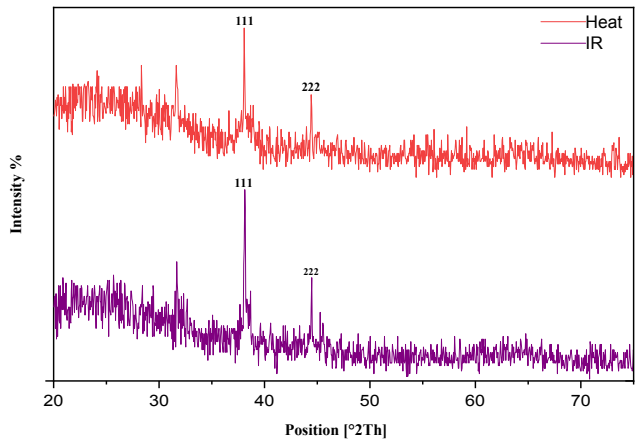

Fig. 6. XRD of the synthesized Au NPs by IR and heat.

Table 1
Particle sizes of the synthesized Au nanoparticles.

D (nm)	β	FWHM	d	Cos θ	2θ	Procedure
16.86	0.0087	0.4994	2.82	0.9451	38.14	Heat
8.78	0.0167	0.9600	2.35	0.9447	38.26	IR

solution may be significantly affected the reduction process by causing the transfer of an electron to the Au atom [58].

The EDX analysis (Fig. 4) showed peaks of Au element, in addition to carbon, oxygen, and sodium arrived from the extract, which indicates organic molecules enclose the synthesized Au NPs [31]. The denoting of the Cl peak can be attributed to $HAuCl_4{\cdot}4H_2O$ salt. It can be observed that the IR procedure yields a high atomic percentage of carbon (33.83%) compared to the heat strategy (31.82%), but a reverse trend is noted for Au. These states may be related to the influence of heat on organic compounds due to the high energy compared with the low energy by IR irradiation.

The Zeta Potential results confirmed that the extract of fresh mature fruits of *P. farcta* is an effective capping and stabilization agent for Au NPs in the colloidal solution. Fig. 5-Heat showed the Zeta Potential value subjected to heat treatment was −25.2 ± 6.23 mV, which was attributable to the good coordination between the extract and nanoparticles. On the other hand, the Zeta Potential value of the Au colloidal solution prepared with the IR strategy was −28.9 ± 9.75 mV (Fig. 5-IR). This slightly higher value of Zeta Potential is due to the high surface area of AuNPs (Figs. 2 and 3) [6] produced via IR, which leads to a more significant impact on the charges spreading around the Au^0, thus preventing the aggregation of NPs.

According to the XRD pattern (Fig. 6), a highly intense Bragg's reflection for the (1 1 1) lattice was observed; suggesting the Au nanoparticles are oriented flat on a planar surface. The main diffraction peak of Au NPs synthesized by heat has been observed at 2θ value of 38.14°, while that Au NPs prepared using IR have been noted at 2θ value of 38.26°. These 2θ values correspond to the planes (1 1 1) of face-centered cubic (FCC) Au metal crystal lattice [18]. The average particle size of the synthesized NPs has been calculated using Debye-Scherrer formula (Eq. (4)):

$$D = \frac{k\lambda}{\beta cos\theta} \tag{4}$$

where D, K, λ, θ and β denote particle diameter size, constant (approximately 0.90), the wavelength of the X-ray utilized (0.15406 nm), Bragg angle and Full Width at Half Maximum (FWHM) values (converted from degree to the radial angle after multiplying it by $\left(\frac{\pi}{180}\right)$), respectively. The particle sizes of the synthesized Au nanoparticles are presented in Table 1.

As observed in Table 1, all particle sizes obtained are in the nanoscale, which confirms the monocrystallinity of Au NPs. The particle size of NPs prepared with IR radiation is smaller than of NPs synthesized by heat. The nanoscale particle size indicates the presence of negative charges on Au NPs, which create a repulsion force that prevents the aggregation of AuNPs. Besides, the IR increases the oscillations and Brownian motion of NPs, which lead to prevent the agglomeration of NPs [61]. It is remarkable to note that the XRD peak position for AuNPs prepared with IR shifted towards higher 2θ values, which was evident in the exchange of the atomic position within Au NPs. However, the broadening of the peak could be attributable to the closely spaced or overlapping peaks due to the presence of impurities in the colloidal solution.

The GC-Mass analysis has been used to diagnose active organic compounds in the *P. farcta* extract, as in Fig. 7. Table 2 indicates the essential molecules (library search report) in the aqueous extract of *P. farcta*, there are 21 compounds that appeared in this extract.

In this study, the FTIR spectrum of *P. farcta* aqueous extract has been analyzed based on the result of GC-Mass, who reported that *P. farcta* is rich in saccharides compounds. As shown in Fig. 8-Extract, there are six distinctive bands (3400 cm^{-1}, 2919 cm^{-1}, 1618 cm^{-1}, 1508 cm^{-1}, 1454 cm^{-1} and 1050 cm^{-1}) in the FTIR spectrum of the prepared extract. The band at 3400 cm^{-1} assigns to overlap the hydroxyl (O—H) stretch and

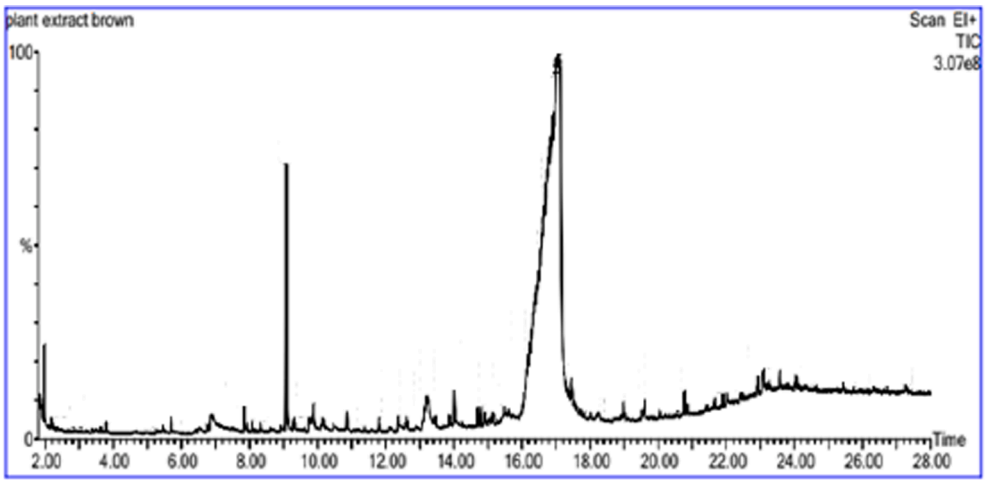

Fig. 7. GC–MS spectra of the *P. farcta* extract.

Table 2
The library search report of expected compounds in the *P. farcta* extract.

No.	Name	Structure
1	Oxirane. 2,3-dimethyl-, trans-(2R,3R)-2,3-dimethyloxirane	
2	Oxirane, 2.3-dimethyl-. cis-(2S,3R)-2,3-dimethyloxirane	
3	methylsilane	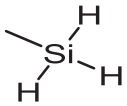
4	acetic acid	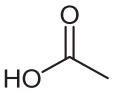
5	Diisooctyl phthalate	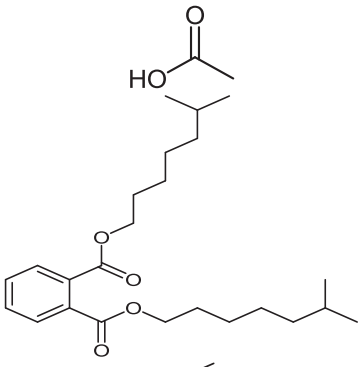
6	Phthalic acid, di(2-propylpentyI) ester	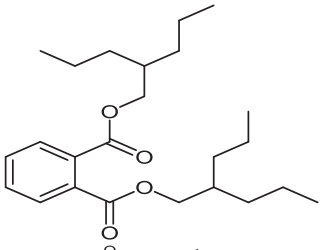
7	4H-Pyran-4-one,2,3-dihydro-3,5-dihydroxy-6-methyl-	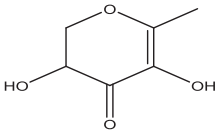
8	2-Propyl-tetrahydropyran-3-ol	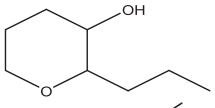
9	1,3-Dioxolane, 2,4,5-trimethyl-	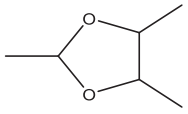
10	2-Tetrazene, 1,1-diethyl-4,4-dimethyl-	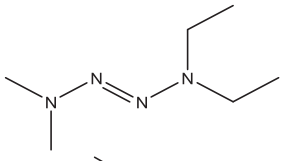
11	3-O-Methyl-d-glucose	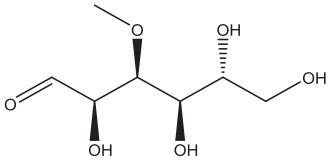
12	a-d-Mannofuranoside, methyl	

Table 2 (*continued*)

No.	Name	Structure
13	myo-inositol, 2-c-methyl-	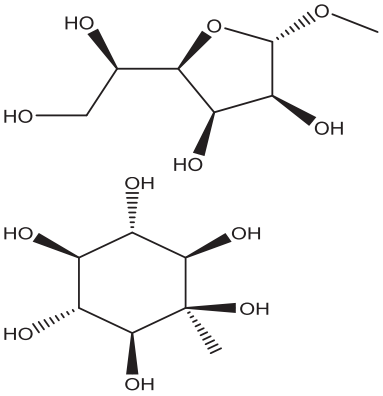
14	Adipamide	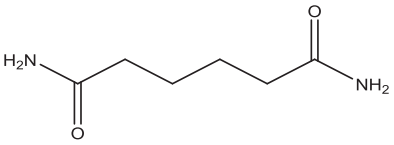
15	Pentanamide, 5-hydroxy-	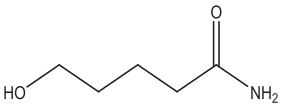
16	Trans-4,5-Epoxynonane	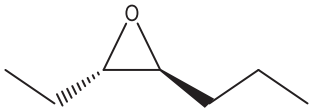
17	1, 1,2-Trimethyl-1-silacyclobutane	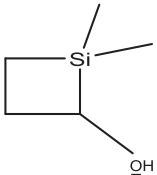
18	d-Glycero-d-galacto-heptose	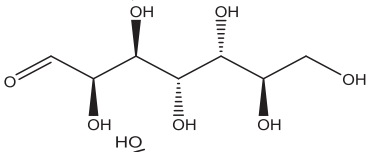
19	2,5-Monomethylene-l-rhamnitol	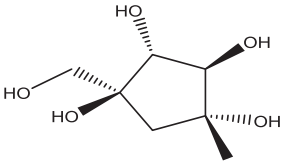
20	L-Glucose	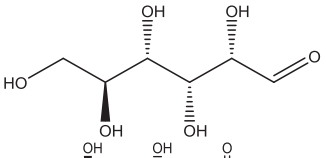
21	Galacto-heptulose	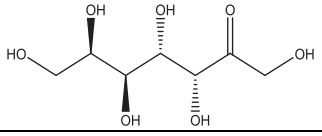

free amide (N–H) stretch. In comparison, the band at 2919 cm^{-1} denotes the presence of —C—H and —CH_2, which indicate aliphatic C—H stretching. The band at 1618 cm^{-1} is related to the stretching vibration of a carbonyl group (C═O), whereas bands at 1508 cm^{-1} and 1454 cm^{-1} signify the amide I and aromatic ring in the extract compounds.

The FTIR spectrum (Fig. 8-Heat) of Au NPs prepared using the heat strategy shows absent aliphatic C—H stretching bond at 2900 cm^{-1} and weak intensity of —OH group at 3400 cm^{-1}, which can be attributed to the evaporation or complete disintegration of organic compounds in

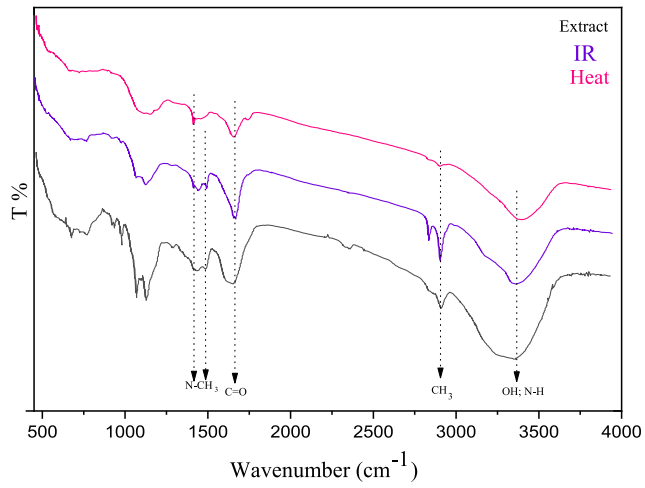

Fig. 8. FTIR spectra of the *P. farcta* extract and the synthesized AuNPs by IR and heat.

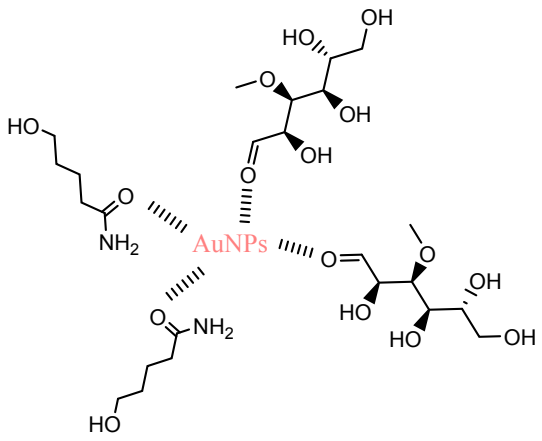

Fig. 9. The excpected gold nanoparticles synthesized from *P. farcta* compounds.

fruits like light compounds from the organic extract by the high temperature [62]. Thus, the FTIR results indicate that IR radiation protects the denaturation of proteins on the surfaces of AuNPs, which is confirmed by the substantial presence of *Prosopis farcta* residues, as indicated by the functional groups of the organic extract at the following bands: 3400 cm^{-1}, 2919 cm^{-1}, 1618 cm^{-1}, 1508 cm^{-1} and 1454 cm^{-1} (Fig. 8-IR). This protection of Au NPs surface coatings has led to higher stability and smaller size by IR compared with the heat treatment. Finally, the expected gold nanoparticles synthesized from *P. farcta* compounds seem as in Fig. 9.

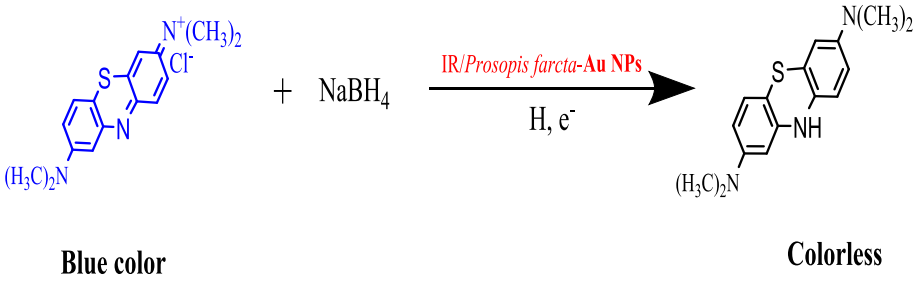

(5)

3.1. Decolonization efficiency of MB

Azo dyes, like methylene blue (MB), are greatly utilized in the textile industry, making one of the most important water pollutants with other dyes [63–65]. Here, the catalytic efficiency of *P. farcta*-AuNPs synthesized by heat and/or IR irradiation has been investigated for the removal of MB (10 ppm) in the presence of $NaBH_4$ (50 μM). The catalytic degradation of the MB has been monitored at an absorption peak of 670 nm (Fig. 10). Similar concentrations of $NaBH_4$ and *P. farcta*-AuNPs have been used to conduct a comparative decolorization study in the presence of AuNPs synthesized using IR and heat treatments as nanocatalysts. Initially, the control treatment of the MB has been applied in the absence of gold nanoparticles to monitor the degradation reactions. The oxidation–reduction reaction between MB dye and $NaBH_4$ has been carried out through the electron relay effect. Electron transfer from $NaBH_4$ to MB involves powerful activation energy, which causes it kinetically difficult to transfer the electron without catalytic effectiveness (Eq. (5)).

Bring the AuNPs in the medium serves as the transition stage (an electron acceptor and an electron donor simultaneously) [66]. *P. farcta*-AuNPs have been used in order to relay electrons from BH_4^- to MB. Fig. 10 refers to the decolorization efficacy of MB with changing volumes of the AuNPs. The photocatalytic degradation of the blue dye exhibits a rapid decrease in intensity over time. This specifically showed the extraordinary effect of *P. farcta*-AuNPs on the decolorization of MB in the presence of a reducing agent. The complete removal of MB has been achieved within 60 sec by a completely eco-friendly method. This can be explained that the small size of *P. farcta*-Au NPs synthesized by IR treatment creates a wide surface area for catalysis process, which agrees with a previous study on photocatalytic activity of AuNPs has shown the relationship between its catalytic performance and the crystallographic size and structure [67]. Also, other studies had been demonstrated prolonged reaction times between Au NPs and dye without a catalyst [68,69]. Although there are no documents on the investigation of IR treatment for fabricated *P. farcta*-Au NPs for the removal of the dye, thus, the results reported in this work are highly important.

Also, Fig. 10 shows the efficacy of the MB photodegradation using *P. farcta*-AuNPs synthesized by IR and heat. These *P. farcta*-AuNPs are gradually leading to degrading MB. The percent removal of MB is

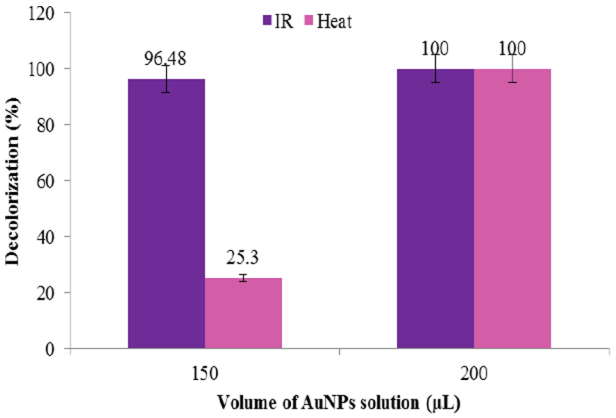

Fig. 10. Decolorization efficacy of MB dye using AuNPs synthesized using IR and Heat after 1 min.

96.48% and 25.30% by using 150 µL AuNPs synthesized by IR and heat, respectively, after 60 sec, while this removal increased to 100% after 60 sec with increasing the volume of AuNPs to 200 µL. Finally, it can be argued that *P. farcta*-AuNPs produced using heat treatment may be considered less efficient in removing MB from aqueous solution compared to *P. farcta*-AuNPs produced by IR light. Furthermore, the biomaterials-assisted mycosynthesis of gold nanoparticles have been used for the decolorization of organic dye [6,31]. Generally, using biomaterials to fabricate new greener nanoparticles is remarkable due to their low toxicity and finding bioactive organic materials around gold atoms [44]. These nanoparticles can be used for many usages which agree with many studies such as using nanomaterials to water treatment [32–34], degradation of organic dyes [35,38–41], reducing pharmaceutical residues [37] and pesticides from wastewater [42].

4. Conclusion

This paper is a new attempt to compare the structural differences between gold nanoparticles (Au NPs) bio-synthesized from the extract of *Prosopis farcta* using infrared (IR) irradiation and heating treatment. Results of the current study indicated that the Au NPs phyto-synthesized using IR radiation characterized by higher colloidal stability, controlled smaller particle size, more spherical morphology and more preserved core–shell structure compared with Au NPs prepared using the heating treatment. This confirms the potential of utilizing IR irradiation successfully to synthesize nanomaterials in the presence of eco-friendly reducing agents like *P. farcta*. Also, Au NPs synthesized by IR radiation exhibited the best decolorization of MB dye compared with Au NPs synthesized by the heat strategy.

CRediT authorship contribution statement

Muwafaq Ayesh Rabeea: Writing – review & editing , Investigation, Formal analysis, Methodology. **Ghassan Adnan Naeem:** Supervision, Writing – review & editing. **Mustafa Nadhim Owaid:** Project administration, Writing – original draft. **Azlan Abdul Aziz:** Data curation, Funding acquisition. **Mahmood S. Jameel:** Validation, Data curation. **Mohammed Ali Dheyab:** Validation, Data curation. **Rasim Farraj Muslim:** Conceptualization, Visualization. **Lina F. Jameel:** Methodology, Resources, Investigation.

Declaration of Competing Interest

The authors declare that they have no known competing financial interests or personal relationships that could have appeared to influence the work reported in this paper.

Acknowledgement

The authors would like to thank School of Physics and Universiti Sains Malaysia for providing characterization tools and funding under FRGS grant 203.PFIZIK.6711768. And a special thank is to Iraqi Ministry of Education to accept this project No. 31406/6/13 registered on 08/08/2019 and Iraqi Ministry of Higher Education and Scientific Research order No. 23649 registered on 17/09/2019.

References

[1] X. Wang, Y. Cao, Characterizations of absorption, scattering, and transmission of typical nanoparticles and their suspensions, J. Ind. Eng. Chem. 82 (2020) 324–332, https://doi.org/10.1016/j.jiec.2019.10.030.
[2] K. Ranoszek-soliwoda, E. Tomaszewska, E. Socha, P. Krzyczmonik, A. Ignaczak, P. Orlowski, M. Krzyzowska, G. Celichowski, J. Grobelny, The role of tannic acid and sodium citrate in the synthesis of silver nanoparticles, J. Nanoparticle Res. 19 (2017) 273, https://doi.org/10.1007/s11051-017-3973-9.
[3] S. Boini, N.R. Barray, N.R. Vajapeyajula, S.A. Koppoli, S.R. Vundrala, B.A. Md, Structural and Morphological Studies of TiO 2 Nanorods synthesized by sonochemical route, Int J Curr Sci Eng Technol. 1 (2018) 49–51. 10.30967/ijcrset.1.1.2018.49-51.
[4] C.S. Estes, A.Y. Gerard, J.D. Godward, S.B. Hayes, S.H. Liles, J.L. Shelton, T. S. Stewart, R.I. Webster, H.F. Webster, Preparation of highly functionalized carbon nanoparticles using a onestep acid dehydration of glycerol, Carbon N Y. 142 (2019) 547–557.
[5] N. Suganthy, V.S. Ramkumar, A. Pugazhendhi, G. Benelli, G. Archunan, Biogenic synthesis of gold nanoparticles from Terminalia arjuna bark extract : assessment of safety aspects and neuroprotective potential via antioxidant, anticholinesterase, and antiamyloidogenic effects, Env. Sci. Pollut. Res. 25 (2018) 10418–10433, https://doi.org/10.1007/s11356-017-9789-4.
[6] S.Y. Abdul-Hadi, M.N. Owaid, M.A. Rabeea, A. Abdul Aziz, M.S. Jameel, Rapid mycosynthesis and characterization of phenols-capped crystal gold nanoparticles from Ganoderma applanatum, Ganodermataceae, Biocatal. Agric. Biotechnol. 27 (2020), 101683, https://doi.org/10.1016/j.bcab.2020.101683.
[7] H. Yang, Y. Ren, T. Wang, C. Wang, Preparation and antibacterial activities of Ag/Ag+/Ag3+ nanoparticle composites made by pomegranate (Punica granatum) rind extract, Results Phys. 6 (2016) 299–304, https://doi.org/10.1016/j.rinp.2016.05.012.
[8] M.R. Vaezi, S.M. Kazemzadeh, A. Hassanjani, A. Kazemzadeh, Effects of ultrasound irradiation time on the synthesis of lead oxide nanoparticles by sonochemical method, J. Optoelectronics Adv. Mater. 17 (2015) 1458–1463.
[9] B.K. Sodipo, A. Abdul Aziz, One minute synthesis of amino-silane functionalized superparamagnetic iron oxide nanoparticles by sonochemical method, Ultrason - Sonochem. 40 (2018) 837–840, https://doi.org/10.1016/j.ultsonch.2017.08.040.
[10] S.K. Srikar, D.D. Giri, D.B. Pal, P.K. Mishra, S.N. Upadhyay, Green Synthesis of Silver Nanoparticles: A Review, Green Sustain. Chem. 06 (01) (2016) 34–56, https://doi.org/10.4236/gsc.2016.61004.
[11] M. Ali, A. Abdul Aziz, M.S. Jameel, P.M. Khaniabadi, B. Mehrdel, Mechanisms of effective gold shell on Fe3O4 core nanoparticles formation using sonochemistry method, Ultrason - Sonochem. 64 (2020), 104865, https://doi.org/10.1016/j.ultsonch.2019.104865.
[12] R.M. Al-Bahrani, S. Muayad, A. Majeed, M.N. Owaid, Phyto-fabrication, characteristics and anti-candidal effects of silver nanoparticles from leaves of Ziziphus mauritiana Lam, Acta Pharm Sci. 56 (2018) 85–92. 10.23893/1307-2080.APS.05620.
[13] M.N. Owaid, T.A. Zaidan, R.F. Muslim, Biosynthesis, Characterization and Cytotoxicity of Zinc Nanoparticles Using Panax ginseng Roots, Araliaceae, Acta Pharm Sci. 57 (2019) 19–32. 10.23893/1307-2080.APS.05702.
[14] R.F. Muslim, M.N. Owaid, Synthesis, characterization and evaluation of the anti-cancer activity of silver nanoparticles by natural organic compounds extracted from Cyperus sp. rhizomes, Acta Pharm Sci. 57 (2019) 129–146. 10.23893/1307-2080.aps.05708.
[15] K. Anand, R.M. Gengan, A. Phulukdaree, A. Chuturgoon, Agroforestry waste moringa oleifera petals mediated green synthesis of gold nanoparticles and their anti-cancer and catalytic activity, J. Industrial Eng. Chem. 21 (2015) 1105–1111, https://doi.org/10.1016/j.jiec.2014.05.021.
[16] M.N. Owaid, Green synthesis of silver nanoparticles by Pleurotus (oyster mushroom) and their bioactivity : Review, Environ. Nanotechnol. Monit Manag. 12 (2019), 100256, https://doi.org/10.1016/j.enmm.2019.100256.
[17] M.N. Owaid, M.A. Rabeea, A. Abdul Aziz, M.S. Jameel, M.A. Dheyab, Mushroom-assisted synthesis of triangle gold nanoparticles using the aqueous extract of fresh Lentinula edodes (shiitake) Omphalotaceae, Environ. Nanotechnol. Monit Manag. 12 (2019), 100270, https://doi.org/10.1016/j.enmm.2019.100270.
[18] M.N. Owaid, G.A. Naeem, R.F. Muslim, R.S. Oleiwi, Synthesis, characterization and antitumor efficacy of silver nanoparticle from Agaricus bisporus pileus, Basidiomycota, Walailak, J. Sci. Technol. 17 (2) (2020) 75–87.
[19] M.N. Owaid, R.F. Muslim, H.A. Hamad, Mycosynthesis of Silver Nanoparticles using Terminia sp Desert Truffle, Pezizaceae, and their Antibacterial Activity, Jordan J. Biol. Sci. 11 (2018) 401–405.
[20] S.K.R. Namasivayam, A.L. Francis, R.S.A. Bharani, C.V. Nachiyar, Bacterial biofilm or biofouling networks with numerous resilience factors from real water supplies of

Chennai and their enhanced susceptibility to biocompatible nanoparticles, J Clean Prod. 231 (2019) 872–898, https://doi.org/10.1016/j.jclepro.2019.05.199.
[21] M.N. Owaid, Silver nanoparticles as unique nano-drugs, in: A.M. Grumezescu, V. Grumezescu (Eds.), Mater Biomed Eng Bioact Mater Prop Appl, 1st Editio, Elsevier, 2019, pp. 545–580.
[22] M. Nasrollahzadeh, M. Sajjadi, J. Dadashi, H. Ghafuri, Pd-based nanoparticles: Plant-assisted biosynthesis, characterization, mechanism, stability, catalytic and antimicrobial activities Mahmoud, Adv. Colloid Interf. Sci. 276 (2020), 102103, https://doi.org/10.1016/j.cis.2020.102103.
[23] M. Nasrollahzadeh, S.M. Sajadi, A. Rostami-vartooni, Journey on greener pathways : use of Euphorbia condylocarpa M. bieb as reductant and stabilizer for green synthesis of Au / Pd bimetallic nanoparticles as reusable catalysts in the Suzuki and Heck coupling reactions in water, RSC Adv. 4 (2014) 43477–43484, https://doi.org/10.1039/C4RA07173E.
[24] N. Motahharifar, M. Nasrollahzadeh, A. Taheri-kafrani, R.S. Varma, M. Shokouhimehr, Magnetic chitosan-copper nanocomposite : A plant assembled catalyst for the synthesis of amino- and N -sulfonyl tetrazoles in eco-friendly media, Carbohydrate Polym. 232 (2020), 115819, https://doi.org/10.1016/j.carbpol.2019.115819.
[25] V.A. Online, S.M. Sajadi, M. Maham, A. Ehsani, Facile and surfactant-free synthesis of Pd nanoparticles by extract of fruits of piper longum and their catalytic performance for Sonogashira coupling reaction in water under ligand- and copper-free conditions, RSC Adv. 5 (2015) 2562–2567, https://doi.org/10.1039/b000000x.
[26] M. Nasrollahzadeh, S.M. Sajadi, Journal of Colloid and Interface Science Green synthesis of Pd nanoparticles mediated by Euphorbia thymifolia L. leaf extract : Catalytic activity for cyanation of aryl iodides under ligand-free conditions, J. Colloid Interf. Sci. 469 (2016) 191–195, https://doi.org/10.1016/j.jcis.2016.02.024.
[27] A. Lateef, S.A. Ojo, J.A. Elegbede, The emerging roles of arthropods and their metabolites in the green synthesis of metallic nanoparticles, Nanotechnol Rev. 5 (2016) 601–622, https://doi.org/10.1515/ntrev-2016-0049.
[28] I.C. Oladipo, A. Lateef, J.A. Elegbede, M.A. Azeez, T.B. Asafa, T.A. Yekeen, A. Akinboro, E.B. Gueguim-Kana, L.S. Beukes, T.O. Oluyide, O.R. Atanda, Enterococcus species for the one-pot biofabrication of gold nanoparticles: Characterization and nanobiotechnological applications, J. Photochem. Photobiol. B Biol. 173 (2017) 250–257, https://doi.org/10.1016/j.jphotobiol.2017.06.003.
[29] I.A. Adelere, A. Lateef, A novel approach to the green synthesis of metallic nanoparticles : the use of agro-wastes, enzymes, and pigments, Nanotechnol. Rev. 5 (2016) 567–587, https://doi.org/10.1515/ntrev-2016-0024.
[30] G.O. Akintayo, A. Lateef, M.A. Azeez, T.B. Asafa, I.C. Oladipo, J.A. Badmus, S. A. Ojo, J.A. Elegbede, E.B. Gueguim-Kana, L.S. Beukes, T.A. Yekeen, Synthesis, bioactivities and cytogenotoxicity of animal fur-mediated silver nanoparticles, IOP Conf. Ser. Mater. Sci. Eng. 805 (2020), 012041, https://doi.org/10.1088/1757-899X/805/1/012041.
[31] M.A. Rabeea, M.N. Owaid, A. Abdul Aziz, M.S. Jameel, M.A. Dheyab, Mycosynthesis of gold nanoparticles using the extract of Flammulina velutipes, Physalacriaceae, and their efficacy for decolorization of methylene blue, J. Environ. Chem. Eng. 8 (2020), 103841, https://doi.org/10.1016/j.jece.2020.103841.
[32] M. Nasrollahzadeh, M. Sajjadi, S. Iravani, R.S. Varma, Green-synthesized nanocatalysts and nanomaterials for water treatment : Current challenges and future perspectives, J. Hazard. Mater. 401 (2021), 123401, https://doi.org/10.1016/j.jhazmat.2020.123401.
[33] M. Nasrollahzadeh, M. Sajjadi, S. Iravani, R.S. Varma, Chemosphere Carbon-based sustainable nanomaterials for water treatment : State-of-art and future perspectives, Chemosphere 263 (2021), 128005, https://doi.org/10.1016/j.chemosphere.2020.128005.
[34] M. Nasrollahzadeh, M. Sajjadi, S. Iravani, R.S. Varma, Starch, cellulose, pectin, gum, alginate, chitin and chitosan derived (nano) materials for sustainable water treatment: A review, Carbohydrate Polym. 251 (2021) 116986, https://doi.org/10.1016/j.carbpol.2020.116986.
[35] S. Naghdi, M. Sajjadi, M. Nasrollahzadeh, K. Yop, S.M. Sajadi, B. Jaleh, Cuscuta reflexa leaf extract me diate d green synthesis of the Cu nanoparticles on graphene oxide/manganese dioxide nanocomposite and its catalytic activity toward reduction of nitroarenes and organic dyes, J. Taiwan Instit. Chem. Eng. 86 (2018) 158–173, https://doi.org/10.1016/j.jtice.2017.12.017.
[36] R.M. Abdelhameed, M. El-shahat, H.E. Emam, Employable metal (Ag & Pd)@ MIL-125-NH 2 @ cellulose acetate fi lm for visible-light driven photocatalysis for reduction of nitro-aromatics, Carbohydrate Polym. 247 (2020), 116695, https://doi.org/10.1016/j.carbpol.2020.116695.
[37] H.E. Emam, M. El-shahat, R.M. Abdelhameed, Observable removal of pharmaceutical residues by highly porous photoactive cellulose acetate @ MIL-MOF film, J. Hazard. Mater. 414 (2021), 125509, https://doi.org/10.1016/j.jhazmat.2021.125509.
[38] A. Omidvar, B. Jaleh, M. Nasrollahzadeh, H. Reza, Chemical Engineering Research and Design Fabrication, characterization and application of GO / Fe 3 O 4 / Pd nanocomposite as a magnetically separable and reusable catalyst for the reduction of organic dyes, Chem. Eng. Res. Des. 121 (2017) 339–347, https://doi.org/10.1016/j.cherd.2017.03.026.
[39] H.E. Emam, H.B. Ahmed, E. Gomaa, M.H. Helal, R.M. Abdelhameed, Recyclable photocatalyst composites based on @ MOF @ cotton for effective discoloration of dye in visible light, Cellulose 27 (2020) 7139–7155.
[40] H.E. Emam, N.M. Saad, A.E.M. Abdallah, H.B. Ahmed, International Journal of Biological Macromolecules Acacia gum versus pectin in fabrication of catalytically active palladium nanoparticles for dye discoloration, Int. J. Biolog. Macromol. 156 (2020) 829–840, https://doi.org/10.1016/j.ijbiomac.2020.04.018.
[41] H.E. Emam, H.B. Ahmed, International Journal of Biological Macromolecules Comparative study between homo-metallic & hetero-metallic nanostructures based agar in catalytic degradation of dyes, Int. J. Biolog. Macromol. 138 (2019) 450–461, https://doi.org/10.1016/j.ijbiomac.2019.07.098.
[42] R.M. Abdelhameed, H. Abdel-gawad, H.E. Emam, Journal of Environmental Chemical Engineering Macroporous Cu-MOF @ cellulose acetate membrane serviceable in selective removal of dimethoate pesticide from wastewater, J. Environ. Chem. Eng. 9 (2021), 105121, https://doi.org/10.1016/j.jece.2021.105121.
[43] L.F. De Freitas, G. Henrique, C. Varca, An Overview of the Synthesis of Gold Nanoparticles Using Radiation Technologies, Nanomater Rev. 8 (2018) 939, https://doi.org/10.3390/nano8110939.
[44] G.A. Naeem, R.F. Muslim, M.A. Rabeea, M.N. Owaid, N.M. Abd-Alghafour, Punica granatum L. mesocarp-assisted rapid fabrication of gold nanoparticles and characterization of nano-crystals, Environ. Nanotechnol. Monit Manag. 14 (2020), 100390, https://doi.org/10.1016/j.enmm.2020.100390.
[45] N.M. Pasiecznik, P.J.C. Harris, S.J. Smith, Identifying Tropical Prosopis Species: A Field Guide, HDRA Publishing, UK, 2004.
[46] A.C. Ezike, P.A. Akah, C.O. Okoli, S. Udegbunam, N. Okwume, C. Okeke, O. Iloani, Medicinal Plants Used in Wound Care: A Study of Prosopis africana (Fabaceae) Stem Bark, Indian J. Pharm. Sci. 72 (2010) 334–339, https://doi.org/10.4103/0250-474X.70479.
[47] A. Al-Aboudi, F.U. Afifi, Plants used for the treatment of diabetes in Jordan: A review of scientific evidence, J. Pharmacol. Biol. 49 (2011) 221–239.
[48] K. Asadollahi, N. Abbasi, N. Afshar, Investigation of the effects of Prosopis farcta plant extract on rat's aorta, J. Med. Plants Res. 4 (2009) 142–147.
[49] F. Harzallah-Skhiri, H. Ben Jannet, Flavonoids Diversification in Organs of Two Prosopis Farcta (Banks & Sol.) Eig. (Leguminosea, Mimosoideae) Populations Occurring in the Northeast and the Southeast of Tunisia, J. Appl. Sci. Res. 1 (2005) 130–136.
[50] F.A. Persia, E. Rinaldini, M.B. Hapon, C. Gamarra-Luques, Overview of Genus Prosopis Toxicity Reports and its Beneficial Biomedical Properties, J. Clin. Toxicol. 6 (2016) 5, https://doi.org/10.4172/2161-0495.1000326.
[51] A. Miri, M. Sarani, M. Rezazade, M. Darroudi, Plant-mediated biosynthesis of silver nanoparticles using Prosopis farcta extract and its antibacterial properties, Spectrochim. Acta Part A Mol. Biomol. Spectrosc. 141 (2015) 287–291, https://doi.org/10.1016/j.saa.2015.01.024.
[52] A. Miri, M. Darroudi, R. Entezari, M. Sarani, Biosynthesis of gold nanoparticles using Prosopis farcta extract and its in vitro toxicity on colon cancer cells, Res. Chem. Intermediates 44 (5) (2018) 3169–3177, https://doi.org/10.1007/s11164-018-3299-y.
[53] S. Salari, S.E. Bahabadi, A. Samzadeh-Kermani, F. Yosefzaei, In-vitro evaluation of antioxidant and antibacterial potential of green synthesized silver nanoparticles using prosopis farcta fruit extract, Iran J Pharm Res. 18 (2019) 430–445. 10.22037/ijpr.2019.2330.
[54] M.S. Jameel, A.A. Aziz, M.A. Dheyab, B. Mehrdel, P.M. Khaniabadi, Rapid sonochemically-assisted green synthesis of highly stable and biocompatible platinum nanoparticles, Surf. Interf. 20 (2020), 100635, https://doi.org/10.1016/j.surfin.2020.100635.
[55] M. Sriramulu, S. Sumathi, Photocatalytic, antioxidant, antibacterial and anti-inflammatory activity of silver nanoparticles synthesised using forest and edible mushroom, Advances in Natural Sci. Nanosci. Nanotechnol. 8 (2017), 045012, https://doi.org/10.1088/2043-6254/aa92b5.
[56] M.N. Owaid, S.S.S. Al-Saeedi, I.A. Abed, Biosynthesis of gold nanoparticles using yellow oyster mushroom Pleurotus cornucopiae var. citrinopileatus, Environ. Nanotechnol. Monit. Manag. 8 (2017) 157–162, https://doi.org/10.1016/j.enmm.2017.07.004.
[57] P. Singh, Y.J. Kim, D.C. Yang, A strategic approach for rapid synthesis of gold and silver nanoparticles by Panax ginseng leaves, Artif. Cell Nanomed. B 44 (8) (2016) 1949–1957.
[58] A. Barth, Infrared spectroscopy of proteins, Biochim Biophys. 1767 (9) (2007) 1073–1101, https://doi.org/10.1016/j.bbabio.2007.06.004.
[59] T.I. Karu, Mitochondrial Signaling in Mammalian Cells Activated by Red and Near-IR Radiation, Photochem Photobiol. 84 (2008) 1091–1099. 10.1111 /j.1751-1097.2008.00394.x.
[60] L.F. de Freitas, M.R. Hamblin, Lucas Freitas Michael Hamblin, Proposed Mechanisms of Photobiomodulation or Low-Level Light Therapy, IEEE J. Selected Topics Quant. Electronics 22 (3) (2016) 348–364, https://doi.org/10.1109/JSTQE.2016.2561201.
[61] M. Zhang, Removal of nanoparticles by flotation processes, J. Environ. Sci. (China) 38 (2015) 168–171, https://doi.org/10.1016/j.jes.2015.10.001.
[62] M.B. Soquetta, L.d.M. Terra, C.P. Bastos, Green technologies for the extraction of bioactive compounds in fruits and vegetables, CYTA - J Food. 16 (1) (2018) 400–412, https://doi.org/10.1080/19476337.2017.1411978.
[63] H.T.S.A.S. Toohi, M.A. Rabeea, J.A. Abdullah, R.F. Muslim, Synthesis and characterization activated carbon using a mix (asphalt-polypropylene waste) for novel azo dye (HNDA) adsorption, Carbon Lett. (2020), https://doi.org/10.1007/s42823-020-00185-3.
[64] M. Dheyab, M. Owaid, M. Rabeea, A. Aziz, M. Jameel, Mycosynthesis of gold nanoparticles by the Portabello mushroom extract, Agaricaceae, and their efficacy for decolorization of Azo dye, Environ Nanotechnology, Monit Manag. (2020), 100312, https://doi.org/10.1016/j.enmm.2020.100312.

[65] M.A. Rabeea, T.A. Zaidan, A.H. Ayfan, A.A. Younis, High porosity activated carbon synthesis using asphaltene particles, Carbon Lett. 30 (2) (2020) 199–205, https://doi.org/10.1007/s42823-019-00086-0.
[66] N. Garg, S. Bera, L. Rastogi, A. Ballal, M.V. Balaramakrishna, Synthesis and characterization of L-asparagine stabilised gold nanoparticles: Catalyst for degradation of organic dyes, Spectrochim. Acta Part A Mol. Biomol. Spectros. 232 (2020) 118126, https://doi.org/10.1016/j.saa.2020.118126.
[67] R. Mata, A. Bhaskaran, S.R. Sadras, Green-synthesized gold nanoparticles from Plumeria alba fower extract to augment catalytic degradation of organic dyes and inhibit bacterial growth, Particuology 24 (2016) 78–86, https://doi.org/10.1016/j.partic.2014.12.014.
[68] T.-D. Nguyen, C.-H. Dang, D.-T. Mai, Biosynthesized AgNP capped on novel nanocomposite 2-hydroxypropyl-βcyclodextrin/alginate as a catalyst for degradation of pollutants, Carbohydrate Polym. 197 (2018) 29–37, https://doi.org/10.1016/j.carbpol.2018.05.077.
[69] P. Zhao, X. Feng, D. Huang, G. Yang, D. Astruc, Basic concepts and recent advances in nitrophenol reduction by gold- and other transition metal nanoparticles, Coordination Chem. Rev. 287114 –136 (2015), https://doi.org/10.1016/j.ccr.2015.01.002.